

Advancements in Liquid Jet Technology and X-ray Spectroscopy for Understanding Energy Conversion Materials during Operation

Published as part of the *Accounts of Chemical Research* special issue “Applications of Liquid Microjets in Chemistry”.

Torben Reuss, Sreeju Sreekantan Nair Lalithambika, Christian David, Florian Döring, Christian Jooss, Marcel Risch, and Simone Techert*



Cite This: *Acc. Chem. Res.* 2023, 56, 203–214



Read Online

ACCESS |

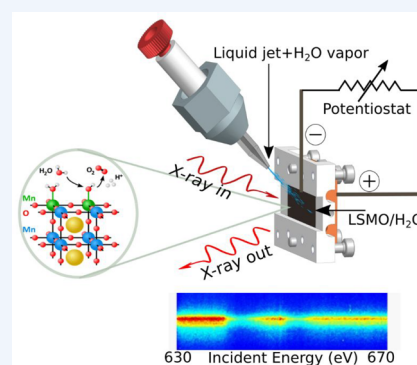
Metrics & More

Article Recommendations

CONSPECTUS: Water splitting is intensively studied for sustainable and effective energy storage in green/alternative energy harvesting–storage–release cycles. In this work, we present our recent developments for combining liquid jet microtechnology with different types of soft X-ray spectroscopy at high-flux X-ray sources, in particular developed for studying the oxygen evolution reaction (OER). We are particularly interested in the development of *in situ* photon-in/photon-out techniques, such as *in situ* resonant inelastic X-ray scattering (RIXS) techniques at high-repetition-frequency X-ray sources, pointing toward *operando* capabilities. The pilot catalytic systems we use are perovskites having the general structure ABO_3 with lanthanides or group II elements at the A sites and transition metals at the B sites. Depending on the chemical substitutions of ABO_3 , their catalytic activity for OER can be tuned by varying the composition.

In this work, we present our *in situ* RIXS studies of the manganese L-edge of perovskites during OER. We have developed various X-ray spectroscopy approaches like transmission zone plate-, reflection zone plate-, and grating-based emission spectroscopy techniques. Combined with tunable incident X-ray energies, we yield complementary information about changing (inverse) X-ray absorption features of the perovskites, allowing us to deduce element- and oxidation-state-specific chemical monitoring of the catalyst. Adding liquid jet technology, we monitor element- and oxidation-state-specific interactions of the catalyst with water adsorbate during OER. By comparing the different technical spectroscopy approaches combined with high-repetition-frequency experiments at synchrotrons and free-electron lasers, we conclude that the combination of liquid jet with low-resolution zone-plate-based X-ray spectroscopy is sufficient for element- and oxidation-state-specific chemical monitoring during OER and easy to handle.

For an in-depth study of OER mechanisms, however, including the characterization of catalyst–water adsorbate in terms of their charge transfer properties and especially valence intermediates formed during OER, high-resolution spectroscopy tools based on a combination of liquid jets with gratings bear bigger potential since they allow resolution of otherwise-overlapping X-ray spectroscopy transitions. Common for all of these experimental approaches is the conclusion that without the versatile developments of liquid jets and liquid beam technologies, elaborate experiments such as high-repetition experiments at high-flux X-ray sources (like synchrotrons or free-electron lasers) would hardly be possible. Such experiments allow sample refreshment for every single X-ray shot for repetition frequencies of up to 5 MHz, so that it is possible (a) to study X-ray-radiation-sensitive samples and also (b) to utilize novel types of flux-hungry X-ray spectroscopy tools like photon-in/photon-out X-ray spectroscopy to study the OER.



KEY REFERENCES

- Hallmann, J.; Grübel, S.; Rajkovic, I.; Quevedo, W.; Busse, G.; Scholz, M.; More, R.; Petri, M.; Techert, S. First steps toward probing chemical reaction dynamics with free-electron laser radiation—case studies at the FLASH facility. *J. Phys. B: At., Mol. Opt. Phys.* **2010**, 43, 194009.¹ *This experimental research paper invents the liquid jet technology for free-electron lasers and demonstrates that the liquid jet can be used in X-ray scattering but also in X-ray*

spectroscopy setups (allowing extension to synchrotron experiments too).

Received: August 4, 2022

Published: January 13, 2023



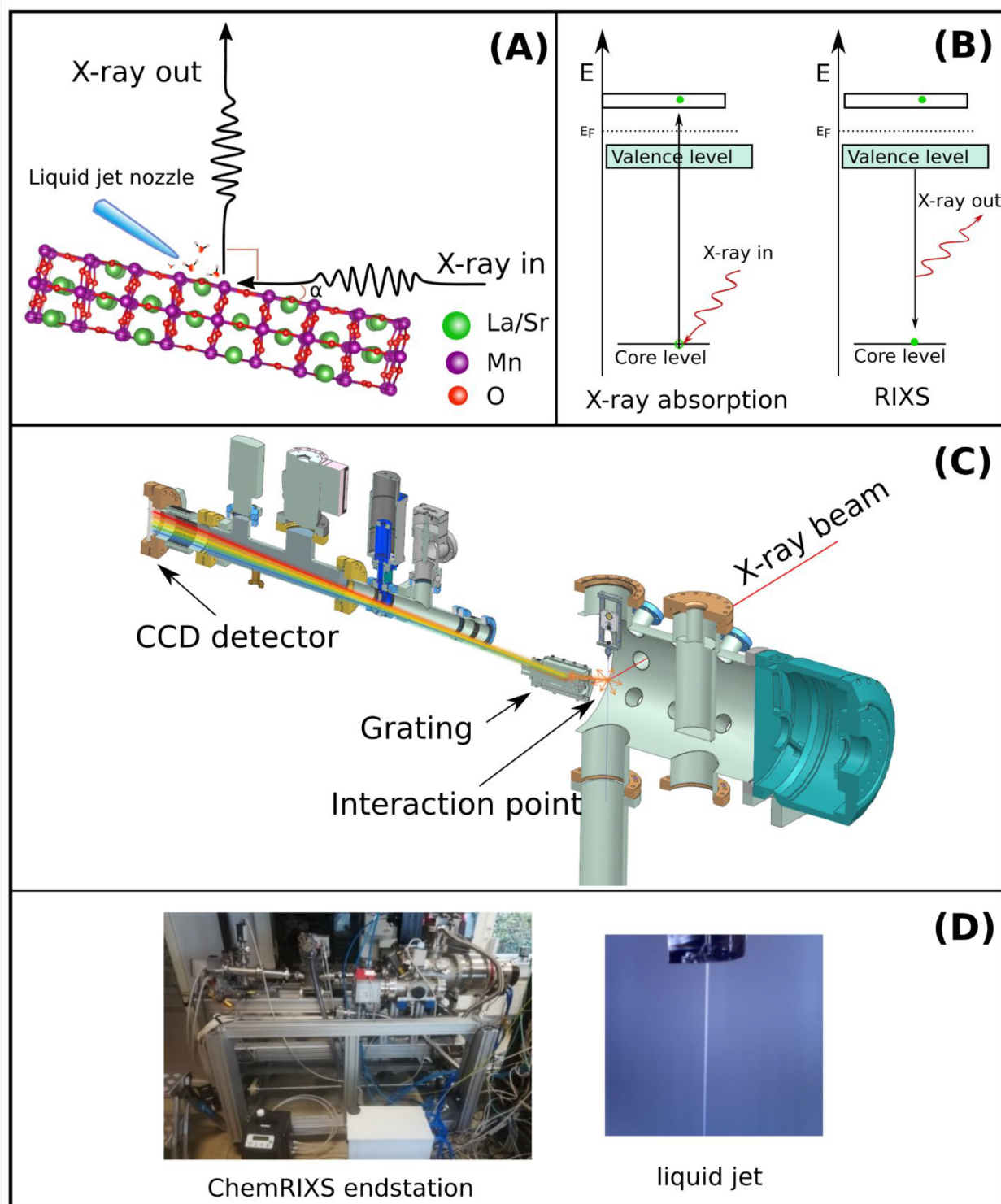


Figure 1. (A, B) Principle of resonant inelastic X-ray scattering (RIXS) and difference between X-ray absorption and RIXS excitation schemes. (C) The ChemRIXS chamber, designed for *in situ* and *operando* studies with ChemRIXS. (D) Photographs of the ChemRIXS chamber and the liquid jet.

- Busse, P.; Yin, Z.; Mierwaldt, D.; Scholz, J.; Kressdorf, B.; Glaser, L.; Miedema, P.S.; Rothkirch, A.; Viehhaus, J.; Jooss, C.; Techert, S.; Risch, M. Probing the surface of $\text{La}_{0.6}\text{Sr}_{0.4}\text{MnO}_3$ in water vapor by *in situ* photon-in/photon-out spectroscopy. *J. Phys. Chem. C* **2020**, *124*, 7893–7902.² This experimental research paper introduces resonant inelastic X-ray scattering at synchrotron sources for surface studies of the electronic properties of complex catalysts. The studies concentrate on perovskites without/with water vapor and confirm former X-ray absorption studies.
- Raabe, S.; Mierwaldt, D.; Ciston, J.; Uijttewaal, M.; Stein, H.; Hoffman, J.; Zhu, Y.; Blöchl, P.; Jooss, C. In situ electrochemical electron microscopy study of oxygen evolution activity of doped manganite perovskites. *Adv. Funct. Mater.* **2012**, *22*, 3378–3388.³ In this work, *in situ*

electron microscopy is introduced for studying perovskite catalysts for the oxygen evolution reaction. Complementary to in situ X-ray spectroscopy, local information about the catalytic activities of the perovskite surface under in situ conditions can be derived.

■ INTRODUCTION

One of the greatest challenges of our current time lies in the systematic research and characterization of chemical reactions that allow the storage and output of energy in a highly efficient manner while conserving natural resources. In the field of the production of so-called “green hydrogen”, the hydrogen evolution reaction (HER) as well as the oxygen evolution reaction (OER), i.e., the production of hydrogen and oxygen by water splitting and its back reaction, belong to the most important and currently most studied chemical reactions of water utilization for energy storage and production.^{4–13} In the field of high-flux X-ray sources, for both synchrotrons and free-electron lasers,¹⁴ this means developing new measurement techniques and methods that provide an alternate and additional view on HER or OER alongside existing measurement techniques, leading to improvements in electrochemically and photoelectrochemically active catalysts and their mode of action.

In soft X-ray spectroscopy, various groundbreaking techniques have been developed for studying OER, focusing on X-ray absorption techniques *in situ*^{15,16} and *operando*.^{17–19} The studies concentrate on detecting the interacting X-rays in absorption mode either by direct transmission absorption experiments or by inverse absorption techniques derived from emission spectra (as explained in the following paragraph). All in all, the X-ray spectroscopies allow monitoring of element-specific oxidation state changes during OER. Insight into hole and electron generation in relation to the band gap properties of the catalytic materials can also be obtained.

With the presented resonant inelastic X-ray scattering (RIXS) experiments we want to add another precision step by determining intermediate species between the catalyst and the water on the surface of the catalyst. To follow the line of already developed techniques, over the last years we have paid particular attention to the development of time-dependent X-ray methods such as time-resolved and ultrafast X-ray diffraction or time-resolved multidimensional soft X-ray spectroscopy for studying chemical reactions beyond X-ray absorption spectroscopy.¹ The development of flux-hungry X-ray spectroscopy techniques to high resolution (Figure 1A) has become possible since we were technically able to couple the liquid jet with its megahertz sample exchange repetition frequency with different photon-in/photon-out X-ray spectrometers. RIXS^{11,12} is a photon-in/photon-out spectroscopy technique where the outgoing energy of photons scattered by the sample is detected as a function of the incident X-ray energy. Figure 1A shows such a photon-in/photon-out scheme on a perovskite sample, one of our pilot systems. Essentially, RIXS is X-ray emission spectroscopy with tuning of the incident X-ray energy. On an atomistic level, the differences between X-ray absorption spectroscopy (XAS) and RIXS are shown in Figure 1B. Staying with the perovskite example, with soft X-ray spectroscopy, the shown generalized transition diagram applies for the transitions and levels involved in RIXS of the oxygen K-edge but also for the transitions and levels involved in the manganese L-edge. For our presented proof-of-concept X-ray spectroscopy studies of the OER, we will concentrate on the X-ray absorption and emission features of the

manganese atoms in $\text{La}_{0.6}\text{Sr}_{0.4}\text{MnO}_3$ (LSMO), i.e., the manganese L-edge transition features, since we expect their oxidation state changes during the OER. The manganese atoms are highlighted as violet points in the LSMO crystal structure shown in Figure 1A. Figure 1B depicts the resonant core excitation (XAS) and subsequent RIXS emission. For transition metals, soft X-rays promote the core 2p electrons directly into the 3d frontier states, which is dipole-allowed. The subsequent decay from the valence states carries the information crucial for understanding the material's physiochemical properties. We yield information about the population of the electronic states of the investigated material (here a perovskite). Combining it with time-resolved *in situ* (or even *operando*) X-ray methods allows changes of the population of the electronic states to be deduced in a dynamic way. Taking into account that RIXS belongs to the core hole clock spectroscopies (Figure 1B), it is possible to gain information about the highest occupied or lowest unoccupied states of the material as well as the corresponding band gaps.

■ SOFT X-RAY EMISSION SPECTROSCOPY DEVELOPMENTS FOR SYNCHROTRONS AND FREE-ELECTRON LASER SOURCES

By tuning the incident X-ray energy and collecting the X-ray emission integrally, or—in other words—inverting XES by monitoring particular X-ray emission spectroscopy (XES) transitions and tuning the incident X-ray energy, it is possible to collect the partial (when partially integrated) fluorescence yield (PFY) and total fluorescence yield (TFY) as functions of the incident energy. The spectra collected are comparable to the ones obtained from X-ray absorption spectroscopy in transmission mode.

However, since the X-ray photons are collected in fluorescence and scattering mode and the X-ray penetration depth sets the monitored sample thickness (Figure 1A), the sample thickness does not define the collected spectra (i.e., via saturation effects),¹ e.g., when the PFY of the 3s to 3d transition is monitored.² It is then possible to study specific selected sheets of layered compositions. An example would be layers on target materials, where the spectroscopic properties of the target materials are out of the monitoring window and thus do not contribute to the background of the collected signals. Furthermore, liquid jets can be added (as another layer), and complex reactions like the OER can be investigated. This finally leads to the possibility of utilizing the full advantages of high-flux X-ray sources (time resolution, high repetition frequency, flux, brilliance, and coherence), allowing for the development of high-resolution and multidimensional X-ray spectroscopy tools like XES or RIXS.^{20–27} This can enable more detailed investigations of the mechanisms driving the OER. Its technical realization is schematically drawn in Figure 1C, and photographs of the setup are shown in Figure 1D. At that time, we named this endstation, which was first operational in 2012 in the soft X-ray regime, the ChemRIXS endstation.^{20–23} In order to reduce background noise in the X-ray spectra, the whole experimental chamber is set to 10^{-3} mbar vacuum, which is a challenge for running the liquid jet smoothly. Radiation damage when monitoring chemical reactions with soft X-ray photons is an additional challenge. To avoid or minimize it, we have developed a vacuum-compatible liquid jet technology.

Since the liquid jet technology (Figure 1D) runs up to megahertz sample exchange rates, ChemRIXS can be coupled to high-repetition-frequency synchrotrons as well as free-electron lasers.^{20–23} ChemRIXS has been operated at PETRA-III,

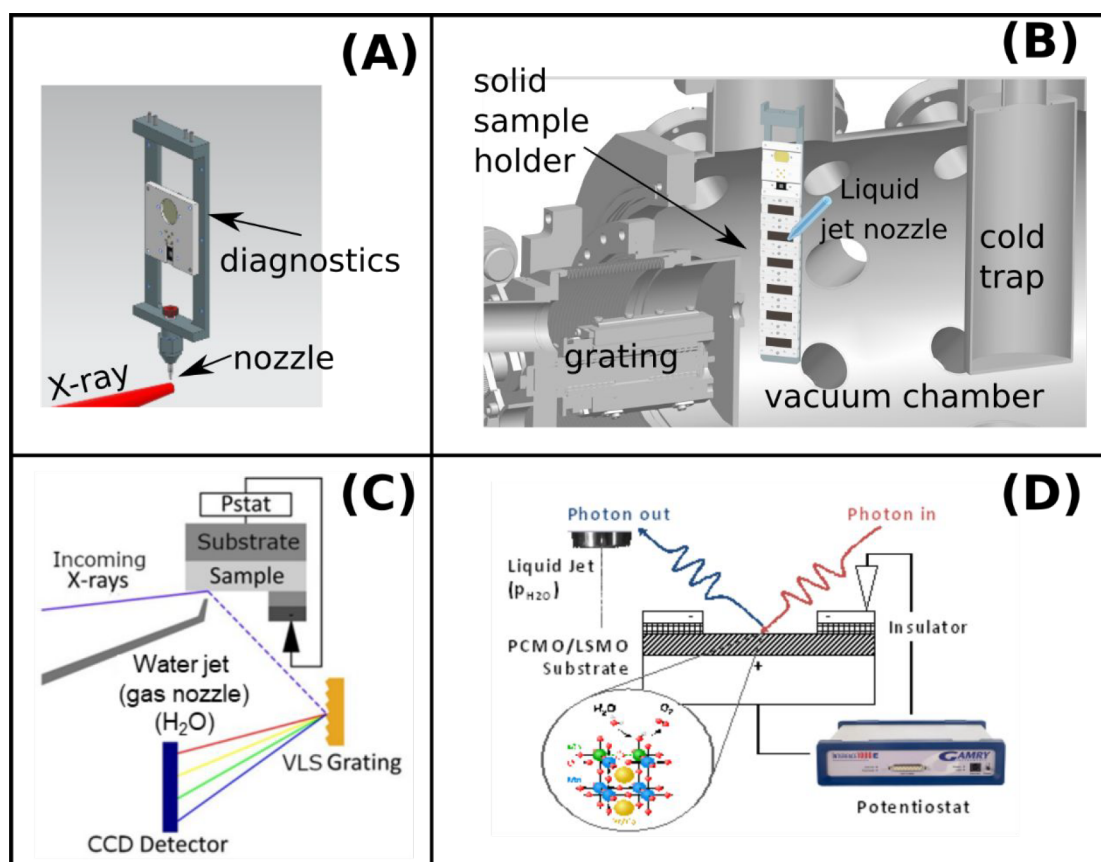


Figure 2. (A) Liquid jet coupling into the ChemRIXS chamber. (B) Liquid jet coupled with surface-sensitive (grazing incidence, GI) X-ray geometry for GIRIXS studies. (C) Design of the ChemRIXS-GIRIXS setup for surface/water/liquids studies, including a potentiostat for *in situ* (and in the future *operando*) GIRIXS studies. (D) Side view of the setup.

FLASH-I, and FLASH-II. The liquid jet is used as a megahertz sample exchange unit in the high-resolution Heisenberg RIXS apparatus at the SCS beamline of the European XFEL.²⁴ The liquid jet technology can avoid typical soft X-ray radiation damage processes that allow otherwise atypical reaction pathways to occur in electrochemistry, which is especially important when studying the reactions of water splitting, namely, HER and OER.

Due to the high-repetition-frequency performance of the liquid microjet and its compatibility with high-flux X-ray sources, we developed the ChemRIXS chamber for time-resolved *in situ* and *operando* studies (Figure 2).^{2,20–23} The multiuse liquid jet (Figure 2A) combines calibration tools with the liquid jet. Furthermore, it is combined with solid-state samples that are active during the OER catalysis (Figure 2B). For possible *in situ* and *operando* studies, the catalysts by themselves are coupled to a potentiostat (Figure 2C,D).^{2,20–23} For *operando* studies, an additional mass spectrometer monitors the catalytic activities. For time-resolved studies in the case of photocatalyst studies, a pulsed optical laser has been coupled in.^{25–27} Time-resolved experiments are reached when external stimuli like a pulsed optical laser are coupled in. Various proof-of-concept studies of this sort have been performed at FLASH and LCLS for XUV and soft X-ray emission spectroscopy, where we determined the electron energy and “real-time movements” (meaning investigating the population changes of electronic states of particular transition energy) in materials, thus contributing to the “film of chemical reactions” from an electron

energy, electron orbital, and electron distribution point of view for molecular and homogeneous catalytic systems.

Due to the flexible geometric design of the various components, it is possible to run the RIXS spectrometers of ChemRIXS in transmission or reflection geometry or in the grazing incidence (GI) geometry as GIRIXS.^{28,29} Our time-resolved *in situ* and *operando* XES/RIXS studies can therefore be either bulk- or surface-sensitive, as shown in Figure 2C,D.

Depending on the information about the OER which we want to gather, different X-ray spectrometer types can be combined with liquid microjets in the ChemRIXS chamber.^{30–34} The exchangeable soft X-ray spectrometer units are equipped with a transmission zone plate (TZP), a reflection zone plate (RZP), and a classical grating spectrometer (Figure 3). Common for all technical approaches of soft X-ray spectroscopy, the XES and RIXS processes consist of the following steps:

- The X-ray beam hits the sample (solid/liquid beam).
- The interaction with the X-rays increases the electron energy in the material/sample under investigation in an element-specific manner.
- The sample emits photons of specific energy.
- The emitted photons hit an optical grating and are separated according to their energies.
- Photons separated according to energy hit the detector.
- A spectrum of energies can be measured via the distribution of photons on the detector.

In ChemRIXS the liquid jet can be combined with a conventional X-ray grating spectrometer, where the incident

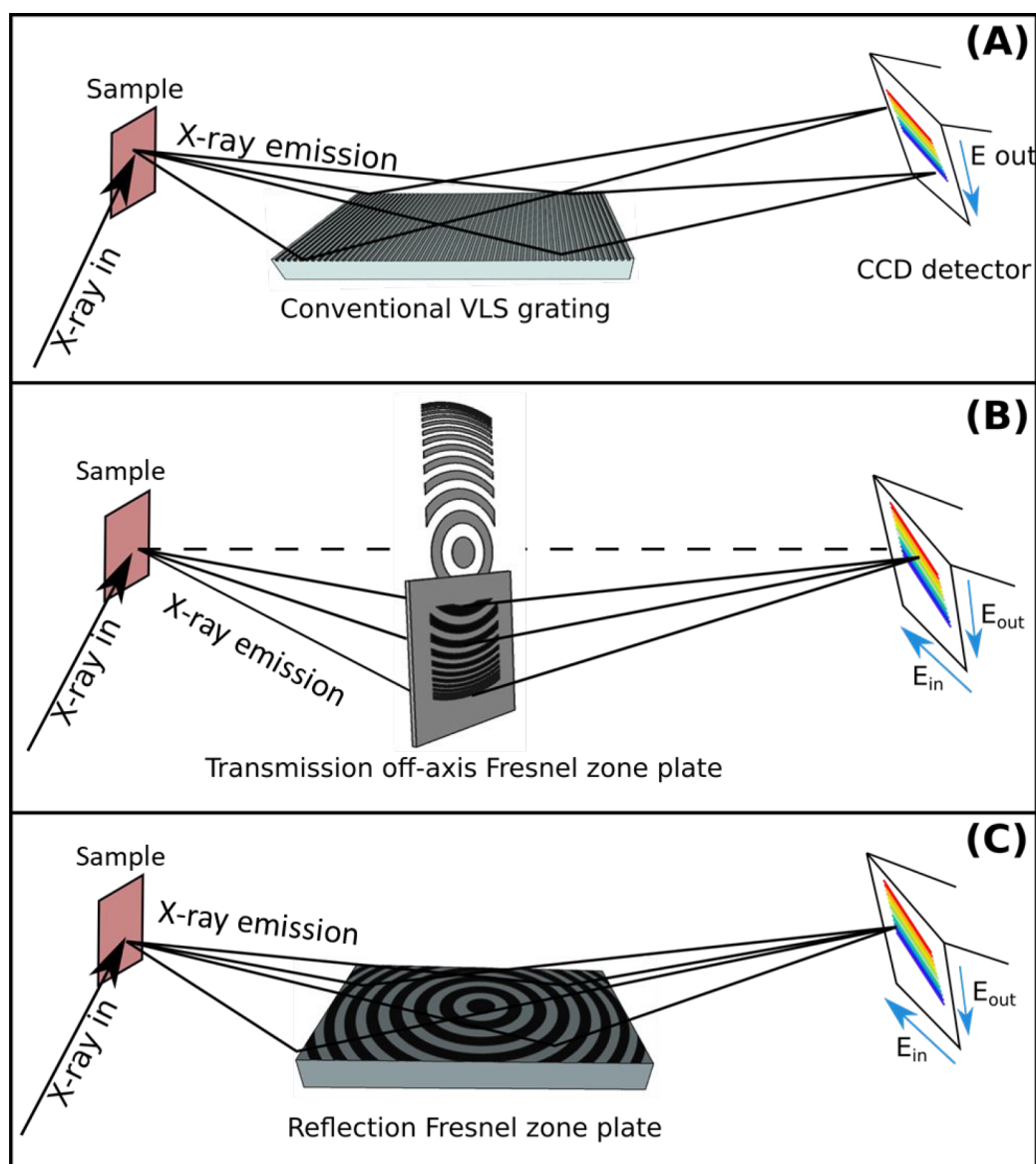


Figure 3. (A) Conventional RIXS detection scheme with a grating. (B) Transmission zone plate for RIXS detection. (C) Reflective zone plate for RIXS detection. All spectrometers can investigate solid-state or liquid bulks or can be operated for grazing incidence recording (GIRIXS). Utilizing the time structure of the high-flux X-ray photon sources (PETRA-III synchrotron and FLASH-I/II free-electron laser) allows for *in situ* and *operando* GIRIXS studies of surfaces with water or other liquids.

X-ray energy is wavelength-selected by a monochromator of the beamline and the outgoing X-ray photons are recorded as XES spectra as a function of incident X-ray energy (Figure 3A). In this way “RIXS maps” can be derived by a stepwise approach of tuning the incident X-ray photon energy and recording the energies of the outgoing X-ray photons scattered from the sample. This conventional way of high-resolution RIXS map collection is only efficient and realizable in a reasonable time window when high-flux X-ray sources with stable photon fluxes are coupled in. Alternatively, when energy resolution issues for the systems investigated are negligible, the recording process can technically be simplified and accelerated by combining the liquid jet with a TZP (Figure 3B) or RZP (Figure 3C), where all sample-emitted X-ray photons are locally selected according to their energies and simultaneously recorded on a 2D X-ray detector.

IN SITU STUDIES ON LSMO/H₂O/KOH INTERFACES

Depending on the scientific question, with these three different types of spectrometers coupled to liquid microjets, different questions of the OER activity and the OER reaction mechanism are addressed. In the following we will present our comparative *in situ* studies of LSMO in water vapor (LSMO*H₂O) and with alkaline solution (LSMO*H₂O/KOH). LSMO perovskite can be used as a catalyst for either the oxygen reduction reaction (ORR) or the OER. Its perovskite crystal structure is shown in Figure 1A.

Perovskite oxides have the general structure ABO₃, where commonly lanthanides or group II elements are found at the A sites and transition metals at the B sites.³⁵ Complete or partial substitution of the A sites and/or B sites changes the physicochemical properties of the perovskite oxide, often without affecting the perovskite structure significantly. Chemical substitutions in perovskite oxides have been shown to impact

their catalytic activity for the OER, making them a good choice for systematic studies.^{36–39} Highly crystalline thin films with defined orientation have been insightful model systems studied in water vapor, e.g., by ambient pressure *in situ* soft XAS,¹⁵ *in situ* XPS/XANES,⁴⁰ environmental TEM,^{3,41–43} or ultrafast time-resolved optical studies.⁴⁴ Here we focus on photon-in/photon-out synchrotron spectroscopy using a liquid jet setup.

In this work we will present the scientific results of two types of proof-of-concept OER studies on LSMO which resemble two complementary X-ray emission spectroscopy capabilities for *in situ* and *operando* studies:

- (i) A study of the OER under *in situ* conditions with low-resolution X-ray emission spectroscopy (Figures 4 and 5). For the qualitative study of the electrochemistry of the bulk catalysts under applied voltage *in situ*, gaseous or liquid jets were coupled to a low-resolution transmission zone plate spectrometer. Additionally, we studied the influence of alkaline solutions on LSMO catalyst properties by analyzing the OER activity of the LSMO*H₂O surface reaction with this low-resolution X-ray emission spectroscopy approach. The studies were also performed adding a mass spectrometer. Since during the experiments no systematic recording was performed (beyond the confirmation of oxygen production), we name the experiments *in situ* rather than *operando* according to the common definitions.
- (ii) A study of the electronic influence of the water adsorbate on the LSMO surface with high-resolution X-ray emission spectroscopy coupled to a liquid jet (Figures 6 and 7). In the high-resolution X-ray experiment, the electronic properties of the LSMO–water surface were studied in detail by coupling the liquid jet to a grating spectrometer. This approach diminished radiation damage issues (like the creation of solvated electrons in the water layer) so that the experiment could run with a megahertz repetition rate. The increase in the rate by 3–5 orders of magnitude allows for high-resolution electronic structure studies, as shown by the X-ray emission/RIXS spectra presented in Figure 7.

In sum, (i) resembles a technical preparation study confirming that LSMO can be studied under *in situ* (or even *operando*) conditions with high-flux X-ray sources. It confirms that spectroscopic analysis deduces trends in manganese oxidation states under *in situ* conditions. The more sophisticated high-resolution *in situ* X-ray emission studies (ii), which are prepared to reduce radiation damage from the high-flux X-ray sources, can be built on the results obtained in (i) and add information about the electronic properties of LSMO when water layers are added for the *in situ* experiments.

Both types of soft X-ray spectrometry allow recording of the changes in the oxidation state or the element-specific chemical composition of the bulk electrocatalyst or water, the surface of the electrocatalyst, or the water adsorbate. In general, the highest surface sensitivity is reached during recording with the grazing incidence geometry.

i. Study of the LSMO OER under *In Situ* Conditions with Low-Resolution X-ray Emission Spectroscopy

For our *in situ* studies, we combined TZP X-ray spectroscopy with a potentiostat and monitored the Mn valence and oxidation states of LSMO with water upon voltage stepping. With the TZP-based X-ray spectroscopy, the changes in the oxidation states of various elements in LSMO can then be quickly

recorded. Integrating in particular the manganese L-edge emission features (3d → 2p_{1/2} RIXS) for different applied voltages yields the manganese L-edge partial fluorescence yields as 3d-PFY. For the iPFY signals we applied the same data procedure as been described in the general procedure of integration of the RIXS features of LSMO.² we obtained the iPFY of the Mn L-edge by integrating the region of interest of the O 2p–1s emission feature and inverting the signal intensity. In the following we will concentrate on the iPFY signals. Changes in (and confirmation of) catalytic activity are additionally monitored by coupling a mass spectrometer to the setup (which is not considered in this work).

On the chemical side, during the OER, water is oxidized to O₂ by the release of electrons, which are given to the LSMO anode surface. At this particular moment of electron admission, higher-valence intermediate Mn states (Mn³⁺/Mn⁴⁺) are formally reduced toward lower-valence states by the admission of electrons, leading to a lower mixed or intermediate valence state (Mn^{2+/3+/4+}). Note that the occurrence of mixed or intermediate valence states of Mn can be distinguished. Intermediate valence states are present in the metallic phases of LSMO, where 3d electrons in the conduction band are delocalized. This is typically the case for valence states in between Mn^{3.2+} and Mn^{3.5+} in highly crystalline LSMO with low defect density. Mixed valence states are present in semi-conducting or insulating phases of LSMO, where electric charge is rather localized and mixed valence states of Mn²⁺, Mn³⁺, and Mn⁴⁺ can evolve. This can be triggered by, e.g., point defects, change of doping, strain, and surface reconstruction. In Figure 4 the iPFY energies have been set through energy calibrations of reference L-edge Mn absorption spectra of defined Mn

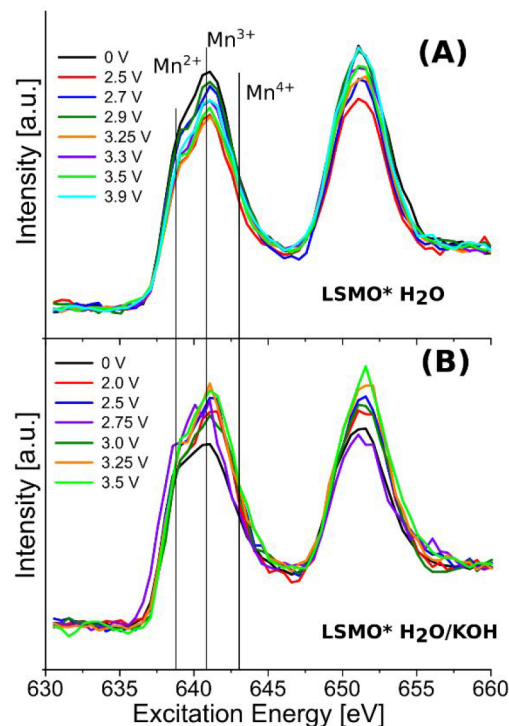


Figure 4. LSMO*H₂O and LSMO*H₂O/KOH surface reactions under voltage steps (vs ground). (A) *In situ* Mn L-edge iPFY of LSMO*H₂O for varying voltages. (B) *In situ* Mn L-edge iPFY of LSMO*H₂O/KOH for varying voltages. The Mn L-edge iPFYs were measured with TZP-GIRIXS spectroscopy.

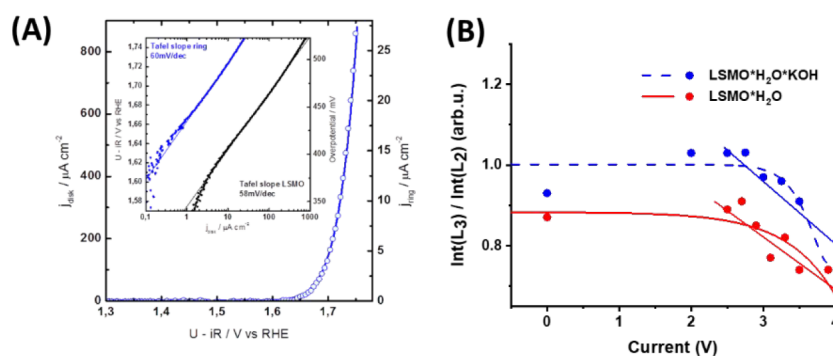


Figure 5. (A) Rotating ring–disk studies of the same LSMO in water system (same doping level, same synthesis approach) emphasizing a voltage threshold at around 1.75–1.8 V vs reversible hydrogen electrode (RHE). The inset shows the LSMO disk and Pt ring detecting oxygen by reduction; the big figure is an overlay of the disk and ring data. (B) iPFY intensity ratio of the Mn-L₃ to Mn-L₂ integral intensities as a function of applied potential. Red curve/line and red circles: LSMO*H₂O. Blue curve/line and blue circles: LSMO*H₂O/KOH.

oxidation states in various manganese oxides,^{15,35,44–48} ranging over the manganese valence states of Mn²⁺, Mn³⁺, Mn^{2+/Mn³⁺}, and Mn⁴⁺. In the current work, the beamline and part of the spectrometers have been calibrated on well-defined argon and xenon lines of soft X-ray gas detectors.^{2,20} This sets the energy of the spectrometers to 0.1–0.5 eV energy precision. The best energy resolution of the TZP, however, is about 0.8–1 eV. Independent of the initial oxidation state, applying Mosley's law yields a +1.6 eV relative shift/oxidation state in our PFY spectra in Figure 4. With the energy resolution of 1 eV in mind, the formal calibration points are the maxima at 639.4 eV for Mn²⁺, 641.4 eV for Mn³⁺ and 643.2 eV for Mn⁴⁺. Additional mixed-state transitions are assigned to the transition shoulders at 639.6 eV (Mn^{2+/Mn³⁺}), 640.5 eV (Mn²⁺), 642 eV (Mn^{2+/Mn³⁺}), and 643.8 eV (Mn⁴⁺), also for mixed valences like in Mn₃O₄.⁴⁶ The assignments of the respective calibration points are marked as vertical lines in the PFY spectra in Figure 4.

The present OER studies of LSMO (as the anode) under more realistic oxidation conditions reveal also a more precise monitoring of the dynamic LSMO oxidation state changes (Figure 4) and suggest that a more complex manganese oxidation state mixture is involved in the LSMO-catalyzed OER. Figure 4 also emphasizes that we already have intermediate/mixed valence states reaching from Mn²⁺ to Mn⁴⁺ in LSMO before the OER and also on the surface. Since also Mn^{2+/Mn³⁺} mixed valence transitions are found at around 639.4 eV and the reference is the zero voltage (vs ground) LSMO form, we interpret the existence of the shoulder and its variation during voltage sweep or surface coverage as a change in the manganese valence state toward smaller values, i.e., from Mn^{3+/4+} to Mn³⁺ or even mixed Mn^{2+/3+} states, etc. It is safe to state that activating LSMO by increasing the applied voltage leads also to a slight reduction of the surface Mn valence states in LSMO, which are not fully recovered by the charge flow back from the bulk and which we will use for the following interpretations as a type of intrinsic LSMO anode feature without water adsorbate and electrolyte around.

Figure 4A shows the *in situ* inverted partial fluorescence yield (iPFY) of LSMO*H₂O, and Figure 4B presents the *in situ* studies of the iPFY of LSMO*H₂O/KOH when the water vapor in the chamber forms a KOH/water mixture with a KOH-covered LSMO film and under voltage sweep. In Figure 4A, the intensity of the iPFY of LSMO*H₂O decreases the first 639 to 643 eV iPFY transition band when the voltage is increased from 0 to 3.9 V, and the second iPFY transition band with its maximum at 652.5 eV increases.

To increase the chemical parameter space of systematic analysis of the OER activity of the electrocatalyst, it is important that the RIXS setup includes additional (chemical experimental) degrees of freedom. Therefore, the studies have been extended from water to alkaline solution covering LSMO. Alkaline solution can be created by either adding water to the salt covering the LSMO surface or using mixing units precoupled to the nozzle and transfer tube for water in a microjet mixing unit that can mix different solution channels, as described previously^{50,51} and shown in Figure 1B. When alkaline solution is added to the LSMO surface, at 0 V vs ground the PFY looks quite similar to the ones of LSMO covered with water without applied voltage potential (Figure 4A). Also here most prominent are the increase of the low-energy transition shoulder of the *in situ* PFY when the voltage is ramped up. Within the resolution of the recorded data, the found behavior is quite similar to that of LSMO covered with water (Figure 4A), suggesting a reduction mechanism similar to that discussed in the case of LSMO*H₂O: when voltage potential is applied, after a specific threshold, again a 639.4 eV transition shoulder appears in the iPFY due to the formation of lower Mn^{2+/Mn³⁺} mixed valence states.

The current spectrometers are not sensitive to eventually fully dissolved Mn ions in water or in alkaline solution (with KOH). The phase evolution at different pH and during oxidation has been previously reported for the Mn-based OER catalysts, and they are found to exhibit high structure flexibility that relates to their OER behavior.⁵²

Formally, the valence state change of Mn can be monitored by calculating the iPFY intensity ratio of the Mn-L₃ to Mn-L₂ integral intensities assuming that the Mn-L₃ edge height is reduced and that other ratios are thus expected for undistorted data. This method has successfully been developed for *in situ* electron energy loss spectroscopy of LSMO for getting a deeper insight into *in situ* studies.^{40,41} Since our PFY spectra are quite distorted (the 3d-PFY even more than the iPFY presented in this work), this analysis can only be seen as a first zeroth-order approach emphasizing the proof of concept of the present study. Figure 5 shows the iPFY intensity ratio of the Mn-L₃ to Mn-L₂ integral intensities as a function of applied potential. The iPFY ratio (Figure 5B) is compared to rotating ring–disk studies on the same system (Figure 5A).⁴⁹ Figure 5B compares the intensity ratios between the L₂ and L₃ edges for LSMO covered with water (LSMO*H₂O) and LSMO covered with alkaline solution (LSMO*H₂O/KOH). For LSMO*H₂O (red curve) and LSMO*H₂O/KOH (blue curve), a clear tendency to a thresholdlike behavior has been found.

In Figure 5B, the ratio onset of LSMO*H₂O is set to 1 for no voltage applied, and that of LSMO*H₂O/KOH is slightly smaller (0.8). The found voltage-independent abscissa offset decreases in the integral intensity ratio of LSMO*H₂O and LSMO*H₂O/KOH can be explained by the decrease of the emitted photon signal due to the added water/alkaline solution layer and the energy-dependent absorption of the added water/alkaline water layer to LSMO.

For both, LSMO*H₂O and LSMO*H₂O/KOH, a voltage threshold of >2.2 V is found, from where the ratio then monotonically decreases as the voltage increases from 2.2 to 4 V vs ground. We hypothesize that the reduction of Mn is due to water/hydroxide oxidation and thus correlate the onset of this reaction with the onset of the OER on LSMO in rotating ring-disk electrode (RRDE) laboratory experiments at 1.65–1.7 V vs RHE, shown in Figure 5A.⁴⁹ The RRDE experiments were performed on the same LSMO system, synthesized in the same way and with the same doping level. The deviations between our found *in situ* studies and the ones from the laboratories can be explained in the following way: first, our proof-of-concept studies presented here are technically not as much optimized as the ring electrode experiments, as already the statistics of both experiments suggest. Second, our applied voltages are not electronically experimentally referenced in the same way as the ring electrode experiments. Third, the ratio method utilizing TZP spectroscopy misses some sensitivity (distorted PFY spectra, etc.) which adds an insensitivity on the ratio scaling (so the ratio changes are detected at higher values than the original ones). Fourth, mechanistic differences may also influence the voltage threshold value since the LSMO sample environment slightly differs in comparison with a ring electrode experiment and the LSMO water layers produced in this experiment. Overall, Figure 5B emphasizes that it is possible with the explained experiment to monitor *in situ* LSMO activity. However, it also emphasizes that more detailed electronic and electronic-structural studies are needed to understand completely the LSMO water coverage.

ii. Study of the Electronic Influence of the Water Adsorbate on the LSMO Surface with High-Resolution X-ray Emission Spectroscopy

When the liquid jet/LSMO is coupled to our high-resolution X-ray emission spectrometer, we can monitor in detail with greater sensitivity the formation of water layers adsorbed on LSMO. From the TZP-based PFY studies explained in the last paragraph, we know that when water is added to the surface but no voltage potential is applied, the valence states of surface Mn are not reduced to pure Mn²⁺ or Mn³⁺ or intermediate Mn²⁺/Mn³⁺ valence states. The discussed inconsistencies and normalization furthermore suggest that there may be more modifications in particular on the LSMO surface that we have not taken into account yet.

With grating-based X-ray spectroscopy and utilizing the megahertz repetition frequency of the synchrotron, RIXS maps of the system can be recorded in a reasonable time. Utilizing the liquid jet reduces the probability of radiation damage. Consequently one RIXS map with the X-ray emission features versus the incident X-ray energy (Figure 6) can be derived which gives a spectral overview over the oxygen K-edge features and the manganese L-edge features (Figure 6) in one map. In the grating experiment, the X-ray transitions between the oxygen K-edge of bulk water and surface water and the ones of the perovskite sublattice in LSMO are well-separated, allowing the

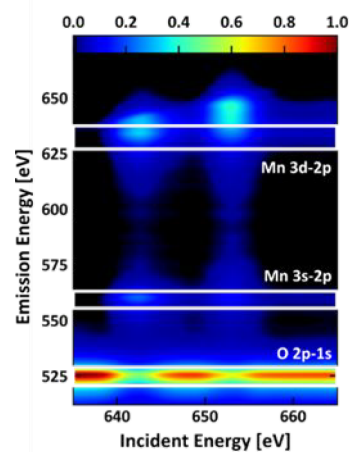


Figure 6. Monitoring of the LSMO*H₂O responses and the electronic properties of LSMO*H₂O. Utilizing the grating spectrometer, the GIRIXS maps of the Mn L-edge and O K-edge of LSMO*H₂O are of higher resolution and allow for the investigation of electronic features beyond an elemental and oxidation state investigation.

partial fluorescence yields of the different oxygen species present in the OER and under the experimental conditions to be distinguished.

Figure 7 presents the high-resolution XES spectrum of the manganese L-edge of LSMO*H₂O recorded with a grating

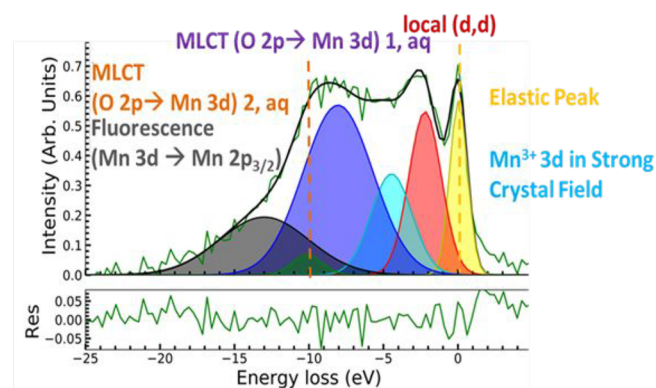


Figure 7. Monitoring of the LSMO*H₂O responses and the electronic properties of LSMO*H₂O. High-resolution XES of LSMO*H₂O recorded with the grating spectrometer allows resolution of charge transfer features between the solvent and LSMO. The color codes are described in the text. The experiment was performed by combining the liquid jet technology with RIXS grating spectroscopy. The excitation energy for this spectrum was set to 642.8 eV.

spectrometer. The XES spectrum can directly be energy-calibrated to the elastic peak (yellow line). Additional different mixed/intermediate Mn³⁺/Mn⁴⁺ valence states can be assigned: the resolved transition bands belong to the local d–d transition (orange transition bands), the Mn 3d → 2p_{1/2} fluorescence (gray transition bands), and some Mn³⁺/Mn⁴⁺ emission bands in the strong crystal field (cyan transition bands). These transitions have also been found in other LSMO XES studies.^{47,48} Upon addition of water to LSMO, in the XES spectrum of Figure 7 particularly for the LSMO*H₂O water adsorbate additional transition bands have been observed that were not recorded in our earlier studies of dry LSMO *in vacuo*.² We assign these additional O 2p → Mn 2p emission transition

bands to charge transfer from the oxygen atom of the adsorbed water to the manganese atoms of the LSMO surface, abbreviated as $MLCT_{aq}$ and highlighted with orange and purple transition bands in Figure 7. These $MLCT_{aq}$ states alter the activation properties of the surface Mn sites in LSMO even before application of a potential.

CONCLUSION

We can conclude that the current advances of liquid jet technology combined with state-of-the-art spectroscopy at high-flux X-ray sources allow the study of the electronic, structural/electronic, and mechanistic properties of metastable states as well as very short-lived intermediates. Liquid jet technology not only contributes to time-resolved studies but can also enhance *in situ* (and *operando*) studies since it reduces the probability of accumulating radiation damage. Depending on the X-ray spectrometer added, qualitative or quantitative chemical analysis, like oxidation state changes or element-specific composition changes, can be monitored *in situ*. Due to additional mixing capabilities, liquid jet technologies add further degrees of freedom for the chemical composition. For an in-depth mechanistic study, however, high-resolution X-ray spectroscopy is of advantage. For studying the water-splitting OER electrocatalytic reaction of LSMO perovskite, high-resolution grating studies allow monitoring of transient charge transfer states, the filling of empty LUMOs of LSMO through the adsorption of water, etc. However, all of these novel experimental approaches are only possible through the versatile developments of liquid jets and liquid beam technologies.

AUTHOR INFORMATION

Corresponding Author

Simone Techert – Deutsches Elektronen-Synchrotron DESY, 22607 Hamburg, Germany; Institute for X-ray Physics, Göttingen University, 37077 Göttingen, Germany;
orcid.org/0000-0002-7549-7651;
Email: simone.techert@desy.de

Authors

Torben Reuss – Deutsches Elektronen-Synchrotron DESY, 22607 Hamburg, Germany
Sreeju Sreekantan Nair Lalithambika – Deutsches Elektronen-Synchrotron DESY, 22607 Hamburg, Germany
Christian David – Paul Scherrer Institute, 5232 Villigen-PSI, Switzerland
Florian Döring – Paul Scherrer Institute, 5232 Villigen-PSI, Switzerland; Present Address: XRnanotech GmbH, 5417 Untersiggenthal, Switzerland
Christian Jooss – Institute of Material Physics, Göttingen University, 37077 Göttingen, Germany
Marcel Risch – Institute of Material Physics, Göttingen University, 37077 Göttingen, Germany; Present Address: Nachwuchsgruppe Gestaltung des Sauerstoffentwicklungsmechanismus, Helmholtz-Zentrum Berlin, Hahn-Meitner Platz 1, 14109 Berlin, Germany;
orcid.org/0000-0003-2820-7006

Complete contact information is available at:
<https://pubs.acs.org/10.1021/acs.accounts.2c00525>

Author Contributions

The manuscript was written through contributions of all authors. All of the authors approved the final version of the

manuscript. CRediT: **Torben Reuss** conceptualization (equal), data curation (equal), investigation (equal), methodology (equal), resources (equal), writing-review & editing (equal); **Sreeju Sreekantan Nair Lalithambika** data curation (equal), formal analysis (equal), investigation (equal), methodology (equal), software (equal), validation (equal), writing-review & editing (equal); **Christian David** conceptualization (equal), methodology (equal), resources (equal); **Florian Döring** investigation (equal), methodology (equal), resources (equal); **Christian Jooss** conceptualization (equal), formal analysis (equal), funding acquisition (equal), investigation (equal), methodology (equal), validation (equal), writing-original draft (equal), writing-review & editing (equal); **Marcel Risch** conceptualization (equal), data curation (equal), formal analysis (equal), funding acquisition (equal), investigation (equal), methodology (equal), resources (equal), validation (equal), writing-original draft (equal), writing-review & editing (equal).

Funding

We gratefully acknowledge funding by the Deutsche Forschungsgemeinschaft (DFG) (217133147/SFB 1073 Project C02). The Initiative and Networking Fund of the Helmholtz Association is gratefully acknowledged (Programs HG-Recruitment, HG-Innovation “ECRAPs”, DSF, CMWS, HG-Innovation “FISCOV”). Financial support by the DFG within the Collaborative Research Center SFB1073 Atomic-Scale Control of Energy Conversion (Project C02), Projektnummer 217133147, is acknowledged. This work received funding from the European Union’s Horizon 2020 Research and Innovation Programme under Marie Skłodowska-Curie Grant Agreement 701647.

Notes

The authors declare no competing financial interest.

Biographies

Torben Reuss graduated in mechanical engineering from the Hochschule für Angewandte Wissenschaften Hamburg in 2018. He is currently working in the Photon Science Division of the Deutsches Elektronen-Synchrotron (DESY), Hamburg, where he is in charge of the liquid jet and spectrometer laboratories. He worked on the design and commissioning of various liquid jet systems coupled to X-ray spectrometers, including the next generation of the ChemRIXS endstation and the HeisenbergRIXS experimental station at the SCS beamline of the European XFEL.

Sreeju Sreekantan Nair Lalithambika received his Ph.D. from Freie Universität Berlin in 2019 on the thesis title Electronic Structure of Cobalt Octahedral Complexes in Aqueous Solution. He is presently a postdoctoral researcher at the Photon Science Division of DESY, studying the electronic structure of catalytic materials using soft X-ray spectroscopy.

Christian David is Group Head of X-ray Nano-Optics at the Laboratory for X-ray Nanoscience and Technologies (LXN) of the Paul Scherrer Institute in Switzerland. His research interest focuses on the micro- and nanofabrication of X-ray optical devices and the development of new methods based on these optics for applications in X-ray imaging and spectroscopy at synchrotron and X-ray free-electron laser sources.

Florian Döring is the founder and CEO of XRnanotech, an award-winning Swiss startup company that develops and fabricates nanostructured X-ray optical elements. Before starting the company in 2020, he was a postdoctoral researcher at the Paul Scherrer Institute in the X-

ray Optics and Applications Group after receiving his Ph.D. at Georg-August University in Göttingen, Germany.

Christian Jooss is a professor of materials physics at the University of Göttingen. His research is focused on complex oxides, i.e., strongly correlated perovskites as an important class of energy materials, and using *in situ* electron microscopy techniques. He is spokesperson of the CRC 1073 on Atomic Scale Control of Energy Conversion.

Marcel Risch leads the Young Investigator Group NOME at Helmholtz-Zentrum Berlin cofunded by the ERC Starting Grant ME4OER. He earned his Ph.D. from Free University Berlin and performed interdisciplinary postdoctoral work at MIT. He is enthusiastic about the knowledge-guided design of electrocatalysts for oxygen and nitrogen electrocatalysis for sustainable fuels such as green hydrogen, harnessing insights from innovative *operando* experiments.

Simone Techert is Leading Scientist within the Photon Science Division of DESY and Professor for Ultrafast X-ray Science at Göttingen University. Her research concentrates on kinetic and time-resolved (ultrafast, *in situ*, *operando*) X-ray methods development for complex chemical systems and reaction studies (like water splitting or photovoltaics) and investigation of the electronic and structural properties and dynamics of (sustainable) functional materials.

ACKNOWLEDGMENTS

The authors thank in particular Jens Viehhaus, Leif Glaser, and Katharina Kubicek for technical support of the new results presented in this Account. Zhong Yin is thanked for his technical support of ChemRIXS for the OER studies. Max Baumung and Philipp Busse are thanked for their contribution in integrating collected RIXS spectra. We acknowledge DESY (Hamburg, Germany), a member of the Helmholtz Association HGF, for the provision of experimental facilities. Parts of the reported research were carried out at PETRA III Beamline P04, FLASH (Beamlines BL1, BL2, BL3/CAMP), and FLASH-II (FL24). The involved X-ray research teams and optical laser teams are acknowledged. Beamtime was allocated for proposals I-2051059, 04/2006 to I-20220013, 04/2022; for a complete list of proposals, see the database. The Helmholtz Association is thanked for continuous financial support, and DESY is thanked for preferred access to X-ray instrumentation (RTIII/POF IV). DESY staff are thanked for their competent help in large-scale-facility technical and computer support.

REFERENCES

- (1) Hallmann, J.; Grübel, S.; Rajkovic, I.; Quevedo, W.; Busse, G.; Scholz, M.; More, R.; Petri, M.; Techert, S. First steps towards probing chemical reaction dynamics with free-electron laser radiation—case studies at the FLASH facility. *J. Phys. B: At., Mol. Opt. Phys.* **2010**, *43*, 194009.
- (2) Busse, P.; Yin, Z.; Mierwaldt, D.; Scholz, J.; Kressdorf, B.; Glaser, L.; Miedema, P. S.; Rothkirch, A.; Viehhaus, J.; Jooss, C.; Techert, S.; Risch, M. Probing the surface of $\text{La}_{0.6}\text{Sr}_{0.4}\text{MnO}_3$ in water vapor by *in situ* photon-in/photon-out spectroscopy. *J. Phys. Chem. C* **2020**, *124*, 7893–7902.
- (3) Raabe, S.; Mierwaldt, D.; Ciston, J.; Uijtewaalt, M.; Stein, H.; Hoffmann, J.; Zhu, Y.; Blöchl, P.; Jooss, C. In situ electrochemical electron microscopy study of oxygen evolution activity of doped manganite perovskites. *Adv. Funct. Mater.* **2012**, *22*, 3378–3388.
- (4) Man, I.; Su, H.; Calle-Vallejo, F.; Hansen, H.; Martínez, J.; Inoglu, N.; Kitchin, J.; Jaramillo, T.; Nørskov, J.; Rossmeisl, J. Universality in oxygen evolution electrocatalysis on oxide surfaces. *Chem. Catal. Chem.* **2011**, *3*, 1159–1165.

- (5) Armstrong, F. Why did Nature choose manganese to make oxygen? *Philos. Trans. R. Soc. B* **2008**, *363*, 1263–1270.
- (6) Gono, P.; Pasquarello, A. Oxygen evolution reaction: bifunctional mechanism breaking the linear scaling relationship. *J. Chem. Phys.* **2020**, *152*, 104712.
- (7) Guan, D.; Ryu, D.; Hu, Z.; Zhou, J.; Dong, C.; Huang, Y.; Zhang, K.; Zhong, Y.; Komarek, A.; Zhu, M.; Wu, X.; Pao, C.; Chang, C.; Lin, H.; Chen, C.; Zhou, W.; Shao, Z. Utilizing ion leaching effects for achieving high oxygen-evolving performance on hybrid nanocomposite with self-optimized behaviors. *Nat. Commun.* **2020**, *11*, 3376.
- (8) Song, J.; Wei, C.; Huang, Z.; Liu, C.; Zeng, L.; Wang, X.; Xu, Z. A review on fundamentals for designing oxygen evolution electrocatalysts. *Chem. Soc. Rev.* **2020**, *49*, 2196.
- (9) Rossmeisl, J.; Qu, Z. W.; Zhu, Z.; Kroes, G. J.; Nørskov, J. K. Electrolysis of water on oxide surfaces. *J. Electroanal. Chem.* **2007**, *607*, 83.
- (10) Conway, B. E.; Salomon, M. Electrochemical reaction orders: applications to the hydrogen- and oxygen-evolution reactions. *Electrochim. Acta* **1964**, *9*, 1599.
- (11) Kobussen, A. G. C.; Broers, G. H. The Oxygen Evolution on $\text{La}_{0.5}\text{Ba}_{0.5}\text{CoO}_3$: Theoretical impedance behaviour for a multi-step mechanism involving two adsorbates. *J. Electroanal. Chem.* **1981**, *126*, 221–240.
- (12) Grimaud, A.; May, K.; Carlton, E.; Lee, Y.; Risch, M.; Hong, W.; Zhou, J.; Shao-Horn, Y. Double perovskites as a family of highly active catalysts for oxygen evolution in alkaline solution. *Nat. Commun.* **2013**, *4*, 2439.
- (13) Rossmeisl, J.; Logadottir, A.; Nørskov, J. K. Electrolysis of water on (oxidized) metal surfaces. *Chem. Phys.* **2005**, *319*, 178–184.
- (14) See the different technical design reports of current and future high-flux X-ray sources and the research projects described therein: SSRF. <https://www-ssrl.slac.stanford.edu/> (accessed 2022-12-06). LCLS. <https://lcls.slac.stanford.edu/> (accessed 2022-12-06). ALS. <https://als.lbl.gov/> (accessed 2022-12-06). APS. <https://www.anl.gov/> (accessed 2022-12-06). CHESS. <https://www.chess.cornell.edu/> (accessed 2022-12-06). NSLS II. <https://www.bnl.gov/nsls2/> (accessed 2022-12-06). LNLS-Sirius. <https://lnls.cnpem.br/home/> (accessed 2022-12-06). SACL. <https://sacla.xfel.jp/?p=312&lang=en> (accessed 2022-12-06). Spring-8. <http://www.spring8.or.jp/en/> (accessed 2022-12-06). NanoTerasu. <https://www.nanoterasu.jp/> (accessed 2022-12-06). HZB. https://www.helmholtz-berlin.de/forschung/quellen/bessy/index_de.html (accessed 2022-12-06). PETRA III. <https://photon-science.desy.de/> (accessed 2022-12-06). PETRA IV. https://www.desy.de/research/facilities_projects/petra_iv/index_eng.html (accessed 2022-12-06). FLASH. <https://flash.desy.de/> (accessed 2022-12-06). European XFEL. <https://www.xfel.eu/> (accessed 2022-12-06). MAXLAB IV. <https://www.maxiv.lu.se/> (accessed 2022-12-06). ESRF-EBS. <https://www.esrf.fr/about/upgrade> (accessed 2022-12-06). SOLEIL. <https://www.synchrotron-soleil.fr/en> (accessed 2022-12-06). ALBA. <https://www.cells.es/en/> (accessed 2022-12-06). Elettra. <https://www.elettra.eu/> (accessed 2022-12-06). FERMI. <https://www.elettra.eu/lightsources/fermi.html> (accessed 2022-12-06).
- (15) Risch, M.; Stoerzinger, K.; Han, B.; Regier, T.; Peak, D.; Sayed, S.; Wei, C.; Xu, Z.; Shao-Horn, Y. Redox processes of manganese oxide in catalyzing oxygen evolution and reduction: An *in situ* soft X-ray absorption spectroscopy study. *J. Phys. Chem. C* **2017**, *121* (33), 17682–17692.
- (16) Xi, L.; Schwanke, C.; Xiao, J.; Abdi, F.; Zaharieva, I.; Lange, K. In situ L-Edge XAS study of a manganese oxide water oxidation catalyst. *J. Phys. Chem. C* **2017**, *121* (22), 12003–12009.
- (17) Braun, A.; Sivula, K.; Bora, D.; Zhu, J.; Zhang, L.; Grätzel, M.; Guo, J.; Constable, E. Direct observation of two electron holes in a hematite photoanode during photoelectrochemical water splitting. *J. Phys. Chem. C* **2012**, *116* (32), 16870–16875.
- (18) Al Samarai, M.; Hahn, A. W.; Beheshti Askari, A.; Cui, Y.-T.; Yamazoe, K.; Miyawaki, J.; Harada, Y.; Rüdiger, O.; DeBeer, S. Elucidation of structure–activity correlations in a nickel manganese oxide Oxygen evolution reaction catalyst by *operando* Ni L-edge X-ray

absorption spectroscopy and 2p3d resonant inelastic X-ray scattering. *ACS Appl. Mater. Interfaces* **2019**, *11* (42), 38595–38605.

(19) Drevon, D.; Görlin, M.; Chernev, P.; Xi, L.; Dau, H.; Lange, K. Uncovering The role of oxygen in Ni-Fe(O₂H₂) electrocatalysts using in situ soft X-ray absorption spectroscopy during the oxygen evolution reaction. *Sci. Rep.* **2019**, *9*, 1532.

(20) Rajkovic, I.; Hallmann, J.; Grübel, S.; More, R.; Quevedo, W.; Petri, M.; Techert, S. Development of a multipurpose vacuum chamber for serial optical and diffraction experiments with free-electron laser radiation. *Rev. Sci. Instrum.* **2010**, *81*, 045105.

(21) Yin, Z.; Rajković, I.; Raiser, D.; Scholz, M.; Techert, S. Experimental setup for high resolution X-ray spectroscopy of solids and liquid samples. *Proc. SPIE* **2013**, *8849*, 88490L.

(22) Yin, Z.; Peters, H. B.; Hahn, U.; Agåker, M.; Hage, A.; Reininger, R.; Siewert, F.; Nordgren, J.; Viefhaus, J.; Techert, S. A new compact VUV-Spectrometer for RIXS studies at DESY. *Rev. Sci. Instrum.* **2015**, *86*, 093109.

(23) Yin, Z.; Peters, H.; Hahn, U.; Gonschior, J.; Mierwaldt, D.; Rajkovic, I.; Viefhaus, J. C.; Jooss, C.; Techert, S. An endstation for resonant inelastic X-ray scattering studies of solid and liquid samples. *J. Synchrotron Rad.* **2017**, *24*, 302–306.

(24) hRIXS Consortium (A. Föhlisch, Ed.). *Technical Design Report of the Heisenberg RIXS@EuropeanXFEL (hRIXS) Endstation as to be operated at the "Spectroscopy and Coherent Scattering (SCS) instrument" at the European XFEL*. https://www.xfel.eu/facility/instruments/scs/index_eng.html (accessed 2022-12-06).

(25) Quevedo, W.; Busse, G.; Hallmann, J.; Moré, R.; Petri, M.; Krasniqi, F.; Rudenko, A.; Tschentscher, T.; Stojanovic, N.; Düsterer, S.; Treusch, R.; Tolkiehn, M.; Techert, S.; Rajkovic, I. Ultrafast time dynamics studies of periodic lattices under free-electron laser radiation. *J. Appl. Phys.* **2012**, *112*, 093519.

(26) Kunnus, K.; Rajkovic, I.; Schreck, S.; Quevedo, W.; Eckert, S.; Beye, M.; Suljoti, E.; Weniger, C.; Kalus, C.; Grübel, S.; Scholz, M.; Nordlund, D.; Zhang, W.; Hartsock, R. W.; Gaffney, K. J.; Schlotter, W. F.; Turner, J. J.; Kennedy, B.; Hennies, F.; Techert, S.; Wernet, P.; Föhlisch, A. A setup for resonant inelastic soft X-ray scattering on liquids at free-electron laser light sources. *Rev. Sci. Instrum.* **2012**, *83*, 123109–17.

(27) Wernet, P.; Kunnus, K.; Josefsson, I.; Rajkovic, I.; Quevedo, W.; Beye, M.; Schreck, S.; Grübel, S.; Scholz, M.; Nordlund, D.; Zhang, W.; Hartsock, R. W.; Schlotter, W. F.; Turner, J. J.; Kennedy, B.; Hennies, F.; de Groot, F. M. F.; Gaffney, K. J.; Techert, S.; Odelius, M.; Föhlisch, A. Orbital-specific mapping of the ligand exchange dynamics of Fe(CO)₅ in solution. *Nature* **2015**, *520* (7545), 78–81.

(28) Yin, Z.; Busse, P.; Mierwaldt, D.; Jooss, C.; Techert, S. *Report of the ChemGIRIXS@DESY Endstation, Commissioned at the PETRA III Synchrotron*; DESY, 2017.

(29) Kaan, A.; Techert, S. *Report of the ChemGIRIXS@DESY Endstation, Commissioned at the FLASH Free-Electron Laser*; DESY, 2019.

(30) Yin, Z.; Rehanek, J.; Löchel, H.; Braig, C.; Buck, J.; Firsov, A.; Viefhaus, J.; Erko, A.; Techert, S. A Highly efficient soft X-ray spectrometer based on reflection zone plate for resonant inelastic X-ray scattering measurements. *Opt. Express* **2017**, *25* (10), 10984.

(31) Marschall, F.; Yin, Z.; Beye, M.; Buck, J.; Döring, F.; Guzenko, V.; Kubicek, K.; Rehanek, J.; Raiser, D.; Rösner, B.; Rothkirch, A.; Veedu, S. T.; Viefhaus, J.; David, C.; Techert, S. Transmission zone plates as analyzers for efficient parallel 2D RIXS-mapping. *Nat. Sci. Rep.* **2017**, *7* (1), 8849.

(32) Yin, Z.; Löchel, H.; Rehanek, J.; Goy, C.; Kalinin, A.; Schottelius, A.; Trinter, F.; Miedema, P.; Jain, A.; Valerio, J.; Busse, P.; Lehmkuhler, F.; Möller, J.; Grübel, G.; Madsen, A.; Viefhaus, J.; Grisenti, R.; Beye, M.; Erko, A.; Techert, S. X-ray spectroscopy with variable line spacing based on reflection zone plate optics. *Opt. Lett.* **2018**, *43* (18), 4390–4393.

(33) Döring, F.; Risch, M.; Rösner, B.; Beye, M.; Busse, P.; Kubiček, K.; Glaser, L.; Miedema, P.; Soltau, J.; Raiser, D.; Guzenko, V.; Szabadics, L.; Kochanek, L.; Baumung, M.; Buck, J.; Jooss, C.; Techert, S.; David, C. A zone-plate-based two-color spectrometer for

indirect X-ray absorption spectroscopy. *J. Synchrotron Radiat.* **2019**, *26* (4), 1266–1271.

(34) Yin, Z.; Inhester, L.; Thekku Veedu, S.; Quevedo, W.; Pietzsch, A.; Wernet, P.; Groenhof, G.; Föhlisch, A.; Grubmüller, H.; Techert, S. Cationic and anionic impact on the electronic structure of liquid water. *J. Phys. Chem. Lett.* **2017**, *8*, 3759–3764.

(35) Breternitz, J.; Schorr, S. What defines a perovskite? *Adv. Energy Mater.* **2018**, *8* (34), 1802366.

(36) Antipin, D.; Risch, M. Trends of epitaxial perovskite oxide films catalyzing the oxygen evolution reaction in alkaline media. *J. Phys.: Energy* **2020**, *2*, 032003.

(37) Scholz, J.; Risch, M.; Wartner, G.; Luderer, C.; Roddatis, V.; Jooss, C. Tailoring the oxygen evolution activity and stability using defect chemistry. *Catalysts* **2017**, *7*, 139.

(38) Stoerzinger, K.; Hong, W.; Azimi, G.; Giordano, L.; Lee, Y.; Crumlin, E.; Biegalski, M.; Bluhm, H.; Varanasi, K.; Shao-Horn, Y. Reactivity of perovskites with water: role of hydroxylation in wetting and implications for oxygen electrocatalysis. *J. Phys. Chem. C* **2015**, *119* (32), 18504–18512.

(39) Forslund, R.; Hardin, W.; Rong, X.; Abakumov, A.; Filimonov, D.; Alexander, C.; Mefford, J. T.; Iyer, H.; Kolpak, A.; Johnston, K.; Stevenson, K. Exceptional electrocatalytic oxygen evolution via tunable charge transfer interactions in La_{0.5}Sr_{1.5}Ni_{1-x}Fe_xO_{4±δ} Ruddlesden-Popper oxide. *Nat. Commun.* **2018**, *9*, 3150.

(40) Mierwaldt, D.; Mildner, S.; Arrigo, R.; Knop-Gericke, A.; Franke, E.; Blumenstein, A.; Hoffmann, J.; Jooss, C. In situ XANES/XPS investigation of doped manganese perovskite catalysts. *Catalysts* **2014**, *4*, 129–145.

(41) Raabe, S.; Mierwaldt, D.; Ciston, J.; Uijtewaal, M.; Stein, H.; Hoffmann, H.; Zhu, Y.; Blöchl, P.; Jooss, C. In situ electrochemical electron microscopy study of oxygen evolution activity of doped Manganite perovskites. *Adv. Funct. Mater.* **2012**, *22* (16), 3378–3388.

(42) Lole, G.; Roddatis, V.; Ross, U.; Risch, M.; Meyer, T.; Rump, L.; Geppert, J.; Wartner, G.; Blöchl, P.; Jooss, C. Dynamic observation of Mn-atom mobility at perovskite oxide catalyst interfaces to water. *Commun. Mater.* **2020**, *1*, 68.

(43) Roddatis, V.; Lole, G.; Jooss, C. In situ preparation of Pr_{1-x}Ca_xMnO₃ and La_{1-x}Sr_xMnO₃ catalysts surface for high-resolution environmental transmission electron microscopy. *Catalysts* **2019**, *9*, 751–755.

(44) Raiser, D.; Mildner, S.; Ifland, B.; Sotoudeh, M.; Blöchl, P.; Techert, S.; Jooss, C. Evolution of hot polaron states with a nanosecond lifetime in a Manganite. *Adv. Energy Mater.* **2017**, *7*, 1602174.

(45) Risch, M.; Stoerzinger, K.; Regier, T.; Peak, D.; Sayed, S.; Shao-Horn, Y. Reversibility of Ferri-/Ferrocyanide Redox during Operando Soft X-ray Spectroscopy. *J. Phys. Chem. C* **2015**, *119* (33), 18903–18910.

(46) Gilbert, B.; Frazer, B. H.; Belz, A.; Conrad, P. G.; Neilson, K. H.; Haskel, D.; Lang, J. C.; Srajer, G.; De Stasio, G. Multiple scattering calculations of bonding and X-ray absorption spectroscopy of manganese oxides. *J. Phys. Chem. A* **2003**, *107* (16), 2839–2847.

(47) Kuepper, K.; Klingeler, R.; Reutler, P.; Büchner, B.; Neumann, M. Excited and ground state properties of LaSrMnO₄: A combined X-ray spectroscopic study. *Phys. Rev. B* **2006**, *74*, 115103.

(48) Agui, A.; Butorin, S. M.; Kaambre, T.; Sathe, C.; Saitoh, T.; Moritomo, Y.; Nordgren, J. Resonant Mn L Emission Spectra of Layered Manganite La_{1.2}Sr_{1.8}Mn₂O₇. *J. Phys. Soc. Jpn.* **2005**, *74* (6), 1772–1776.

(49) Scholz, J.; Risch, M.; Stoerzinger, K.; Wartner, G.; Shao-Horn, Y. C.; Jooss, C. Rotating ring-disk electrode study of oxygen evolution at a perovskite surface: correlating activity to manganese concentration. *J. Phys. Chem. C* **2016**, *120* (49), 27746–27756.

(50) Jain, R.; Burg, T.; Petri, M.; Kirschbaum, S.; Feindt, H.; Steltenkamp, S. S.; Sonnenkalb, S.; Becker, S.; Griesinger, C.; Menzel, A.; Techert, S. Efficient microchannel device for scattering experiments with high flux X-ray sources and their perspective towards application in neutron scattering science. *Eur. Phys. J. E* **2013**, *36*, 109.

(51) Jain, J.; Techert, S. Time-resolved and in situ X-ray scattering methods beyond photoactivation: utilizing high-flux X-ray sources for

the study of ubiquitous non-photon active proteins. *Protein Pept. Lett.* **2016**, *23*, 242–254 (part of the special Issue “Synchrotron Applications in Life Science”).

(52) An, H.; Chen, Z.; Yang, J.; Feng, Z.; Wang, X.; Fan, F.; Li, C. An Operando-Raman study on oxygen evolution of manganese oxides: Roles of phase composition and amorphization. *J. Catal.* **2018**, *367*, 53–61.

Recommended by ACS

Early Microjet Experimentation with Liquid Water in Vacuum

Manfred Faubel.

JANUARY 31, 2023

ACCOUNTS OF CHEMICAL RESEARCH

[READ](#) 

Core-Level Photoelectron Angular Distributions at the Liquid–Vapor Interface

Rémi Dupuy, Hendrik Bluhm, *et al.*

JANUARY 25, 2023

ACCOUNTS OF CHEMICAL RESEARCH

[READ](#) 

Origin of the Liquid/Gaseous Water Binding Energy Splitting Measured via X-ray Photoelectron Spectroscopy

Jian Liu, Zhi Liu, *et al.*

JANUARY 19, 2023

THE JOURNAL OF PHYSICAL CHEMISTRY LETTERS

[READ](#) 

UV Photoelectron Spectroscopy of Aqueous Solutions

William G. Fortune, Helen H. Fielding, *et al.*

NOVEMBER 28, 2022

ACCOUNTS OF CHEMICAL RESEARCH

[READ](#) 

[Get More Suggestions >](#)